Influence of ambient pressure on properties and expansion of laser-induced plasma

Yongqiang Zhang (张永强), Chuansong Chen (陈传松), Xinling Zhou (周新玲), Juan Guo (郭 娟), Qinggang Zhang (张庆刚), and Baoyuan Man (满宝元)

College of Physics and Electronics, Shandong Normal University, Ji'nan 250014

Received April 17, 2006

A Nd:YAG pulsed laser is used to ablate HgCdTe target at different ambient pressures, the emission spectrum is detected by a time- and space-resolved diagnostic technique. It is found that the characteristics of time-resolved emission spectra are influenced by the pressure of background gas. A theoretical model is developed to investigate expansion mechanism of plasma, the time evolution of the propagation distances and the velocities of plasma plume are calculated by the model at pressures of 1.01×10^5, 1000, and 5 Pa, respectively. The calculated results are well consistent with the experimental data.

OCIS codes: 300.6500, 020.3690, 010.1320, 000.4430.

When a pulsed laser is focused on a solid surface, it can cause the removal of material by melting, vaporization, sublimation, and a number of nonlinear processes. So far a lot of new physical phenomena have been discovered and many new physical laws have been achieved owing to the use of the pulsed laser with high power density and short duration[1,2]. Nevertheless the interaction between laser and material is very complex, it depends not only on the laser parameters, but also on the ambient pressure[3]. So the further study on the interaction process is necessary.

To date we have carried out the studies on laser ablation of Al and Cu under various pressure conditions[4,5] and have found that the expansion of the plume of the ejected matter can be very affected by the collision between the laser-ablated particles and the background gas. For HgCdTe, as a kind of optimum material for infared detector, we also have made some primary investigation[6]. Next our research group are going to prepare HgCdTe thin film by the pulse laser deposition (PLD) technique. Therefore it is very helpful to further study the characteristic of HgCdTe plasma for getting high quality film.

In the present work, a time- and space-resolved diagnostic technique is used to study the emission spectra from the plume produced by a pulsed laser ablation of a HgCdTe target at different ambient pressures. In order to further study the mechanism of the laser-HgCdTe interaction, the propagation characteristic of the plasma along the normal direction of the target surface has to be known. It has been found in a series of experiments that the propagation of species in plasma can be described by the point-source blast wave model[7,8] and the adiabatic model[9,10]. But the former is valid under a limiting condition that the mass of the gas surrounded by the shock wave is greater than the initial explosion mass. The latter is only applied to describe the laser plasma expansion at low pressure. We have developed a shock wave model first considering the ejected HgCdTe mass in our previous work[6]. In this paper, a new expansion model including radiation energy, ionization energy and the work due to compressing air is established on the basis of previous studies. The calculated propagation distances and velocities of the plasma using the model are well consistent with experiment results.

The arrangement of the experimental apparatus has been schematically shown in Ref. [11]. The pulsed laser used in the experiment is a Nd:YAG laser (Spectra Physics Quanta-Ray DCR-3) and operates in a Q-switched mode. The laser output has a pulse duration of 10 ns and a wavelength of 1.06 μm, and the maximum laser energy is 1 J. The laser energy is measured by a digital energy meter (OPHIR DGX-30A). The laser pulse is focused onto the polished HgCdTe target surface by a quartz focus lens L1 ($f = 6.3$ cm). The focus of the lens is adjusted on the target surface, and the spot size of the laser beam is 0.66 mm in diameter. The HgCdTe sample is positioned on a sample holder in a pumped chamber. Residual air in the chamber is used as buffer gas. The chamber and lens L1 are mounted on two-dimensional (x-y directions) movable plates, respectively. y direction is in the laser beam axis. In x direction, two cylindrical lenses (L2 and L3) are used to image, at 1:1, the plasma emission from the plane which has a distance d from the surface of the target, onto the entrance of the slit of an ISA (HR-320) spectrum analyzer. The dispersed emission is subsequently detected with a 10-ns gated, image-intensified optical multichannel analyzer (PARC OMA III). An accurate trigger delayer, which is synchronistically triggered by the electric Q-switched signal produced from the YAG laser device, is used to control the delay time. In addition, a photodiode and a digitizing oscilloscope (Tektronix TDS620A) are used to calibrate the time delay. By changing the distance d and the delay time $t_{\rm d}$, one can get the space- and time-resolved emission spectra.

The temporal evolution of the emission line profiles in wavelength ranging from 372 to 626 nm at an observation distance of $d = 1.0$ mm from the target surface is shown in Fig. 1, the laser power density is 1.7×10^9 W/cm^2, and the ambient pressures are 1.01×10^5 Pa (Fig. 1(a)) and 5 Pa (Fig. 1(b)). In Fig. 1, both the strong analytical emission lines and an intense background continuum are generated within 10 ns after the laser reaches the

1671-7694/2006/080493-04 http://www.col.org.cn

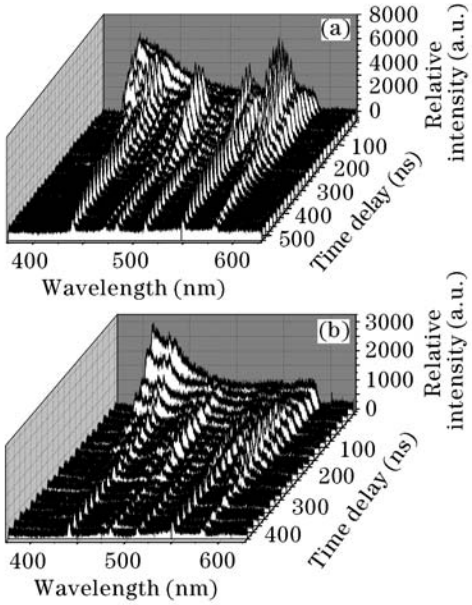

Fig. 1. Temporal evolution of the emission spectra in wavelength ranging from 372 to 626 nm, recorded at 1.0 mm position from the target surface, the ambient pressures are 1.01×10^5 Pa (a) and 5 Pa (b), respectively.

target surface. They all decrease quickly with time delay and almost disappear after 300 ns. It is well known that the continuum is related to the strong collision between free electrons and excited atoms or ions known as bremsstrahlung, and the recombination of electrons and ions, so we can speculate that there must be many electrons, atoms, and ions near the surface of the ablated HgCdTe and the plasma has come into being.

There exist some differences by comparing Figs. 1(a) and (b). Firstly, the lines obtained at 1.01×10^5 Pa last for longer time than those at 5 Pa. The reason is that the ambient air has a stronger confining effect on the plasma at high pressure than at low pressure, which would keep the plasma in high temperature and high density state for a longer time at high pressure. Secondly, we find the corresponding line intensity in Fig. 1(a) is stronger than that in Fig. 1(b). This is because that the increased pressure slows the velocities of the atoms by the collision between air particles and the ejected atoms, thus at low pressure the plasma travels with a higher velocity for lack of impedance and passes the observed position with less time. Finally, from Fig. 1 the spectral line broadening is observed evidently in the initial stage of the plasma plume expansion. The mechanism of the line broadening has been investigated[11] and proved that it resulted dominantly from Stark effect.

The emission intensity of excited atoms is proportional to the number of the excited atoms, and the time delays embody the velocities of the atoms, so time and spatial resolutions reflect the velocity distributions of the excited atoms. Based on the delay time, the maximum intensity for each offset can be used to estimate the velocity. Dividing the distance between the two measured positions by the corresponding difference of the delay time gives the average velocity of the excited atoms. The results at three different ambient pressures under the same experimental conditions are shown in Fig. 2, it can be found

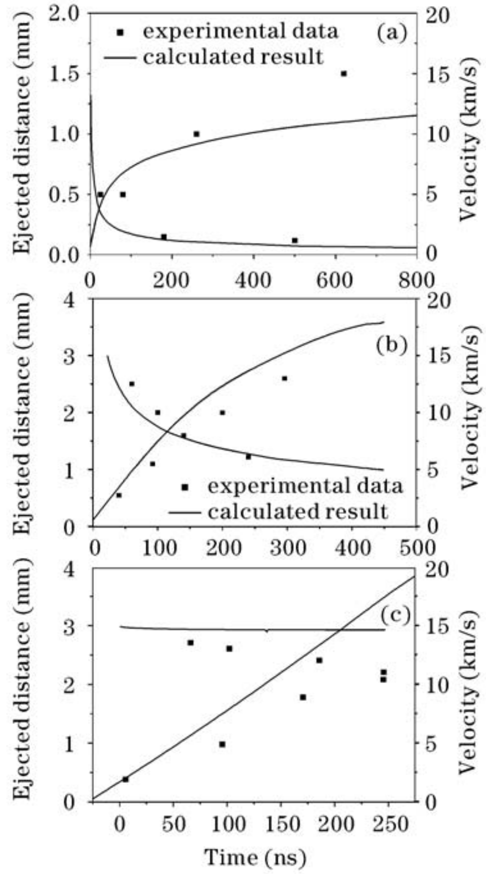

Fig. 2. Comparison of the calculated results and experimental data of the ejected distances and velocities at different pressures of 1.01×10^5 Pa (a), 1000 Pa (b), and 5 Pa (c).

that the velocities decrease with the time delay and reach the level of sound velocity after hundreds of nanoseconds. Furthermore, the velocities of the atoms decrease with time delay more rapidly at higher pressure than at lower pressure. It is because that the increased pressure slows the velocities of the atoms by the collisions between air particles and the ejected atoms. The ejected distance is also given in this figure.

A shock wave model for investigating the propagation of the plasma is developed as follows. In this model, the plasma travels forward with a hemispherical shape pulse and compresses the background gas like a piston, so that all the ejected particles are concentrated near the boundary of the compressed air layer. It is considered that the plasma travels along with the compressed air with the same velocity and temperature.

Let R be the distance of shock wave from detonation point, ΔR be the thickness of the expanding plasma. Both of them are the function of the time of the plasma propagating. Then

$$V = 2\pi R^2 \Delta R, \tag{1}$$

$$S_1 = \pi R^2, \tag{2}$$

$$S_2 = 2\pi R^2, \tag{3}$$

$$D = \frac{\mathrm{d}R}{\mathrm{d}t}, \tag{4}$$

$$V' = \frac{2}{3}\pi R^3, \quad (5)$$

where V is the volume of the plasma, S_1 the interface area of the plasma and the target, S_2 the whole surface area of the shock wave, D the velocity of shock wave front, t the time of plasma expanding, V' the volume of the air compressed by plasma.

In the following we can obtain the relationship between ΔR and t by fitting the experimental values in Ref. [6],

$$\Delta R = 0.347t^{0.195} - 0.422\,(\text{mm}) \quad (1.01\times10^5 \text{ Pa}), (6)$$

$$\Delta R = 0.597t^{0.222} - 0.803\,(\text{mm}) \quad (1000 \text{ Pa}), \quad (7)$$

$$\Delta R = 0.787t^{0.211} - 1.055\,(\text{mm}) \quad (5 \text{ Pa}), \quad (8)$$

the unit of t is ns.

Let P, ρ, and T be the pressure, density, and temperature of the plasma respectively, $E_{\rm K}$ the kinetic energy of the plasma, $E_{\rm T}$ the thermal energy, $E_{\rm I}$ the ionization energy, and $q(t)$ the power of the plasma absorbing energy.

According to the energy conservation laws, we can get

$$\frac{\rm d}{{\rm d}t}(E_{\rm T}+E_{\rm K}) + PDS_1 + \sigma T^4(S_1+S_2) + \frac{{\rm d}E_{\rm I}}{{\rm d}t} = q(t), \quad (9)$$

where $\sigma = 5.67\times10^{-8}$ W/(K^4·m^2) is Stefan-Boltzman constant, PDS_1 is the power used for compressing ambient gas and $\sigma T^4(S_1+S_2)$ is the lost power owing to thermal radiation. Let N_1 be the number of particles of the ejected HgCdTe in the expansion plume and N_2 be the number of compressed air, then the total number of particles N can be obtained as

$$N = N_1 + N_2 = \frac{2m_0}{A_1}N_{\rm A} + \frac{2V'\rho_0}{A_2}N_{\rm A}, \quad (10)$$

where m_0 is the ejected HgCdTe mass, which can be measured by using a profilograph[6], A_1 the molecular weight of HgCdTe, A_2 the molecular weight of air, $N_{\rm A}$ the Avogadro constant, and ρ_0 the density of air. It is assumed that the ejected HgCdTe and the compressed air are dissociated completely into single atom, this approximation could be a good description of the system, because the temperature of plasma is very high.

The total thermal energy of the plasma is

$$E_{\rm T} = \frac{3}{2}NkT, \quad (11)$$

k is Boltzman parameter.

Substituting Eq. (10) into Eq. (11), we get

$$\frac{{\rm d}E_{\rm T}}{{\rm d}t} = \frac{3}{2}k(N_1+N_2)\frac{{\rm d}T}{{\rm d}t} + \frac{3}{2}k\left(\frac{{\rm d}N_1}{{\rm d}t} + \frac{2\rho_0 N_{\rm A}}{A_2}\cdot\frac{{\rm d}V'}{{\rm d}t}\right). \quad (12)$$

The relationship between T and t can be obtained by fitting the experiment results in Ref. [11] as follows

$$T = 2.754\times10^{14}t^{-1.018} + 560\,(\text{K})\ (1.01\times10^5 \text{ Pa}), \quad (13)$$

$$T = 2.509\times10^{14}t^{-1.070} + 765\,(\text{K})\ (1000 \text{ Pa}), \quad (14)$$

$$T = 2.060\times10^{14}t^{-1.102} + 802\,(\text{K})\ (5 \text{ Pa}). \quad (15)$$

The total kinetic energy can be written as

$$E_{\rm K} = \frac{1}{2}mD^2 = \frac{1}{2}(m_0+\rho_0 V')D^2.$$

Differentiating the formula above with respect to time, then

$$\frac{{\rm d}E_{\rm K}}{{\rm d}t} = (m_0+\rho_0V')D\frac{{\rm d}D}{{\rm d}t} + \frac{1}{2}\rho_0 D^2\frac{{\rm d}V'}{{\rm d}t}. \quad (16)$$

Similarly, we can get

$$\frac{{\rm d}E_I}{{\rm d}t} = \frac{2\alpha\rho_0 N_{\rm A}\Sigma_2}{A_2}\cdot\frac{{\rm d}V'}{{\rm d}t} + \left(\frac{2m_0N_{\rm A}\Sigma_1}{A_1} + \frac{2\rho_0V'N_{\rm A}}{A_2}\Sigma_2\right)\cdot\frac{{\rm d}\alpha}{{\rm d}t}, \quad (17)$$

where $\Sigma_1 = 9.576$ eV and $\Sigma_2 = 14.545$ eV are the ionization energies of HgCdTe and nitrogen respectively, α is the ionization coefficient of the plasma. For simplicity, the ejected HgCdTe and the compressed air are considered to be with the same ionization coefficient.

In our model, as in Ref. [12]

$$\alpha = \sigma_{\rm k}\overline{v}P_{\rm D}, \quad (18)$$

where $\sigma_{\rm k} = 10^{-15}$ cm^2 is the gas dynamics section area, $\overline{v}$ is the average thermal velocity and $\overline{v} = \sqrt{\frac{8kT}{\pi m}}$ for Maxwell distributions, $P_{\rm D}$ is the dissociated probability while colliding, $P_{\rm D} \approx {\rm e}^{-\frac{Q}{kT}}$ and $Q = 9.8$ eV, owing to air mostly made up of nitrogen, here we can replace $P_{\rm D}$ of air with that of nitrogen in Eq. (18). So we can obtain

$$\alpha = \sigma_{\rm K}\overline{v}{\rm e}^{-\frac{Q}{kT}}. \quad (19)$$

In addition, we have to apply transient momentum conservation to achieve the shock wave equation because of the effect of dissociation. Then we can obtain

$$(P-P_0)S_1\Delta t - \frac{2\alpha\rho_0S_1D\Delta tN_{\rm A}}{A_2D}\Sigma_2 = \rho_0 D\Delta t S_1 D,$$

$$P = P_0 + \frac{2\alpha\rho_0N_{\rm A}}{A_2}\Sigma_2 + \rho_0D^2, \quad (20)$$

where P_0 is the ambient gas pressure.

The laser power for Gaussian distributions can be described as

$$P(t) = \frac{q_0\tau_{\rm p}}{\sigma\sqrt{2\pi}}{\rm e}^{-\frac{(t-\frac{1}{2}\tau_{\rm p})^2}{2\sigma^2}},$$

where $\sigma = \tau_p/\sqrt{8\ln 2}$, q_0 is the average laser power and $\tau_{\rm p}$=10 ns is the laser pulse width, the reflectivity of the HgCdTe crystal is $r = 0.31$, then the average power of the plasma absorbing laser energy is

$$q(t) = (1-r)P(t). \quad (21)$$

Now all the parameters of Eq. (9) are described as the function of time t and site R, then we can obtain a differential coefficient equation by substituting all equations above into Eq. (9). Obviously resolving this equation by numerical resolution method, we can get the variation of R as a function of t. In the calculation the values of $A_1 = 310$, $A_2 = 29$, $q_0 = 3.89 \times 10^6$ W are used, and the values of 1.25×10^{-3}, 1.25×10^{-5}, and 6.25×10^{-8} g/cm^3 are taken as the densities ρ_0 of air at different pressures of 1.01×10^5, 1000, and 5 Pa, respectively.

From the figures above we can see that the ejected distances and the velocities of the plasma are greatly influenced by the ambient pressure. With the time increasing, the ejected distances increase and the velocities decrease, also at low pressure the velocities decrease more slowly and the distances increase more quickly than those at high pressure during the initial course of the plasma plume expansion. It is evident that the calculated results are well consistent with the experimental data, especially at high pressure and short delay time. At low pressure or long delay time the calculated results are deviated from the experimental data. The reason is that a strong shock assumption has been used in the model. As known to us that a strong shock wave can easily be formed at a high ambient pressure within a short delay time and the assumption is not completely satisfied at low pressure or long delay time. Thus the model that we have established is more suitable for the plasma plume expansion at high ambient pressure and short delay time than at low pressure or long delay time.

At the same time, the ejected distance as a function of time for ambient pressure of 1.01×10^5 Pa can be deduced by fitting the curve line of the calculated results in Fig. 2(a),

$$R = 0.045t^{0.43} + 0.42\,(\mathrm{mm}). \quad (22)$$

The comparison of the ejected distance calculated in our model with the radius of strong shock wave in Ref. [13] shows that they vary similarly with increasing time except for the index of the time. Our result is slightly larger than that of Sedov[14] $R = (\frac{E_0}{\alpha\rho})^{\frac{1}{5}} t^{\frac{2}{5}}$ and smaller than that of Gupta[13] $R(t) \propto t^{0.68}$.

In conclusion, the spectroscopic analysis method is used to investigate the time-resolved behavior of the laser plasma produced from a HgCdTe target at different pressures. The emission characteristics are found to depend strongly on the pressure of the surrounding gas. These results show that the line broadening increases with the pressure increasing and the spectral lines obtained at high pressure last for a longer time than those at low pressure. Furthermore we develop a shock model describing the propagation of the plasma, the calculated ejected distances and the velocities are well consistent with the experimental data, especially at high pressure and short delay time. The results are somewhat deviated from the measured values probably due to the assumption of a strong shock at low pressure or long delay time.

This work was supported by the National Natural Science Foundation of China (No. 10474059, 10474060), the Provincial Natural Science Foundation of Shandong (No. Y2003A01), and the Project Sponsored by SRF for ROCS, SEM, China. B. Man is the author to whom the correspondence should be addressed, his e-mail address is byman@sdnu.edu.cn.

References

1. W. Kong, Y. Zhao, T. Wang, J. Shao, and Z. Fan, Chin. Opt. Lett. **3,** 181 (2005).
2. X. Li, Z. Lin, X. Liu, Y. Chen, S. Gong, Acta Opt. Sin. (in Chinese) **24,** 1051 (2004).
3. S. Amoruso, R. Bruzzese, N. Spinelli, R. Velotta, M. Vitiello, and X. Wang, Phys. Rev. B **67,** 224503 (2003).
4. B. Man, G. Wang, A. Liu, and X. Wang, Spectroscopy and Spectral Analysis (in Chinese) **118,** 411 (1998).
5. Q. Dong, B. Man, Q. Zhang, and X. Wang, Chin. J. Atomic and Molecular Phys. (in Chinese) **18,** 45 (2001).
6. B. Y. Man, X. T. Wang, and A. H. Liu, J. Appl. Phys. **83,** 3509 (1998).
7. W. K. A. Kumuduni, Y. Nakayama, Y. Nakata, T. Okada, and M. Maeda, J. Appl. Phys. **74,** 7510 (1993).
8. Z. Jiang, K. Takayama, K. P. B. Moosad, O. Onodera, and M. Sun, Shock Waves **8,** 337 (1998).
9. S. I. Anisimov, D. Bauerly, and B. S. Luk'yanchuk, Phys. Rev. B **48,** 12076 (1993).
10. T. N. Hansen, J. Schou, and J. G. Lunney, Appl. Phys. A **69,** (Suppl.) 601 (1999).
11. B. Y. Man, Appl. Phys. B **67,** 241 (1998).
12. J. W. Bond, Jr., K. M. Watson, and J. A. Welch, Jr., *Atomic Theory of Gas Dynamics* (in Chinese) X. Fu (trans.) (Science Press, Beijing, 1986) p.356.
13. A. Gupta, B. Braren, K. G. Casey, B. W. Hussey, and R. Kelly, Appl. Phys. Lett. **59,** 1302 (1991).
14. J. Grun, J. Stamper, C. Manka, J. Resnick, R. Burris, J. Crawford, and B. H. Ripin, Phys. Rev. Lett. **66,** 2738 (1991).